AGU **ADVANCING EARTH AND SPACE SCIENCE**

Geophysical Research Letters

Key Points:

- We define piecewise evolutionary spectra (special case of evolutionary spectra) to quantify time-varying second moments in a warming climate
- We introduce ensemble periodograms derived from a large ensemble as consistent estimators of piecewise evolutionary spectra
- We find time-dependent and timescale-dependent changes in relations between NAO and surface temperature

Supporting Information:

Supporting Information may be found in the online version of this article.

Correspondence to:

D. A. Putrasahan,
dian.putrasahan@mpimet.mpg.de

Piecewise Evolutionary Spectra: A Practical Approach to Understanding Projected Changes in Spectral Relationships Between Circulation Modes and Regional Climate Under Global Warming

D. A. Putrasahan[1] and **J.-S. von Storch[1,2]**

[1]Max Planck Institute for Meteorology, Hamburg, Germany, [2]Center for Earth System Research and Sustainability (CEN), Universität Hamburg, Hamburg, Germany

Abstract Regional climate variability is strongly related to large-scale circulation modes. However, little is known about changes in their spectral characteristics under climate change. Here, we introduce piecewise evolutionary spectra to quantify time-varying variability and co-variability of climate variables, and use ensemble periodograms to estimate these spectra. By employing a large ensemble of climate change simulations, we show that changes in the variability and relationships of the North Atlantic Oscillation (NAO) and regional surface temperatures are disparate on individual timescales. The relation between NAO and surface temperature over high-latitude lands weakens the most on 20-year timescales compared to shorter timescales, whereas the relation between NAO and temperature over subtropical North Africa strengthens more on shorter timescales than on 20-year timescales. These projected evolution and timescale-dependent changes shed new light on the controlling factors of circulation-induced regional changes. Accounting for them can lead to the improvement of future regional climate predictions.

Plain Language Summary Large-scale atmospheric circulation modes influence regional climate variability. For example, the North Atlantic Oscillation (NAO) is a circulation mode closely linked to surface temperatures variations over Europe, Africa, and North America. However, under global warming, changes in regional climate variability and their relation to circulation modes (co-variability) can evolve differently and disparately depending on timescales. Here, we use the theory of evolutionary spectra to quantify these nonstationary changes and present a novel approach to estimate such changes on various timescales. The estimation approach is based on a large ensemble of climate change simulations. We show that changes in the NAO and regional surface temperature variability and their relationships evolve differently on individual timescales. On 20-year timescales, co-variability between NAO and surface temperature weakens over high-latitude lands surrounding the northern North Atlantic, whereas the corresponding co-variability on shorter timescales strengthens over subtropical North Africa. These differing evolution and timescale-dependent changes shed new light on the controlling factors of circulation-induced regional changes. Taking them into account can lead to the improvement of future regional climate predictions.

1. Introduction

Large-scale circulation modes directly influence regional climate variability. A prominent example is the North Atlantic Oscillation (NAO) which substantially influences climate variability over Europe, Africa, and North America. It is well-known that during the wintertime, a positive phase of the NAO leads to warmer and wetter than normal conditions in northern and western Europe and the eastern coast of the United States, and cooler and drier conditions in eastern Canada, western Greenland, and northern parts of Africa (Hurrell, 1995; Hurrell & Deser, 2009; Hurrell et al., 2003). With increasing greenhouse gas (GHG) concentration, not only circulation modes and their relations to regional climate can change (Deser et al., 2017), their relations can also change in different ways on different timescales. Knowledge about how these relations on different time scales change with increasing GHG concentration is essential for improving our understanding of regional climate change and eventually improving regional projection and prediction. This paper examines the timescale-dependent changes in the relation between NAO and

surface temperatures by estimating the evolution of their spectra using an ensemble of 1% CO_2-increase-per-year climate change simulations from the Max Planck Institute-Grand Ensemble (MPI-GE) (Maher et al., 2019). Unlike a multi-model ensemble, such a single-model ensemble excludes variability introduced by inter-model uncertainties (Deser et al., 2012; Maher et al., 2018). The ensemble consists of 100 ensemble members. Each ensemble member is initialized from a coupled climate state taken from a 2000-years pre-industrial control (PI-control) run.

Quantifying changes between circulation modes and regional climate faces two major difficulties, both of which can be dealt with using large ensembles. First, being more closely linked to the dynamics than thermodynamics, circulation changes are much more difficult to detect than thermodynamic changes, such as those related to the global mean temperature and sea level (Shepherd, 2014). Deser et al. (2012) showed that the weak signals in circulation changes could be detected using a large ensemble. Second, a fundamental cause of a nonstationary climate system is the time-dependency of external forcings, such as an increasing CO_2 concentration. Quantifying time-dependent statistics for such a system is difficult when using a single realization, but straightforward when using an ensemble. To ensure a high accuracy of these estimates, a large ensemble is required.

Science based on large ensembles has advanced in recent years (e.g., Deser et al., 2012; Fyfe et al., 2017; Kay et al., 2015; Kolstad & Screen, 2019; Manzini et al., 2018; Rodgers et al., 2015). The idea of using large ensembles to quantify temporal changes in statistics (e.g., variances or co-variances) of a nonstationary warming climate has been appreciated and adopted (Maher et al., 2019; Milinski, 2019). However, much less has been explored regarding changes in spectra for a nonstationary system. It is not clear how a non-stationary spectrum should be defined, at least within the climate change community. In this study, we use piecewise evolutionary spectra (PES), a particular case of evolutionary spectra, to evaluate the evolution of spectra of a nonstationary system and show how to use a large ensemble of climate change simulations to estimate such spectra. We apply this technique to investigate: (a) how the variability of NAO and surface temperatures on different timescales change and (b) how the relationship between NAO and surface temperatures on various timescales change with increasing GHG concentration.

## 2. Piecewise Evolutionary Spectra

2.1. PES as a Special Case of Priestley's Evolutionary Spectra

The theory of spectral analysis virtually applies only to stationary processes. Nonstationary processes are usually dealt with by removing nonstationary features like trends from the first moment. For quantifying non-stationarity in second moments, a more general theory of spectral analysis is needed. Such a theory—that of *evolutionary spectra* (ES)—is proposed by Priestley (1965) and Priestley (1967, 1981, 1988) and briefly summarized in Section A of the supporting information (S1). We propose to consider a case of ES, named piecewise evolutionary spectra (PES).

Priestley's ES is defined for oscillatory processes that can be represented by oscillatory functions, ϕ, in the form of complex exponential functions (sine or cosine waves) with modulating amplitudes that vary *extremely slowly* with time. In the present study, Priestley's consideration for continuous oscillatory processes (see SI-A.1) is translated to discrete oscillatory processes, X_n, defined at integer time steps n. The evolutionary spectral density, $h_n(\omega)$, at frequency ω and time step n can be determined by the variance of Y_n, a process representing a general linear transformation of X_n. Consider a realization of X_n, denoted as x_n with $n = 0, ..., N-1$, then the realization of the linear transformation of x_n, which is y_n, is given by

$$y_{n,\omega_j} = \frac{1}{N} \sum_{m=n-N+1}^{n} g_m \, x_{n-m} \, e^{-i\omega_j(n-m)}. \tag{1}$$

g_m is a digital filter with a characteristic width and different weights at different time steps m. If x_n is a realization of a stationary X_n, then y_n obtained from Equation 1 using a filter g_m with unit weights throughout the entire time domain corresponds to the Fourier coefficient of x_n at frequency ω_j. Priestley showed that for a narrow enough g much smaller than the characteristic width of ϕ, and for h much smoother than the transfer function of the filter g, h is approximately given by the variance of Y (see SI-A.1). When translated
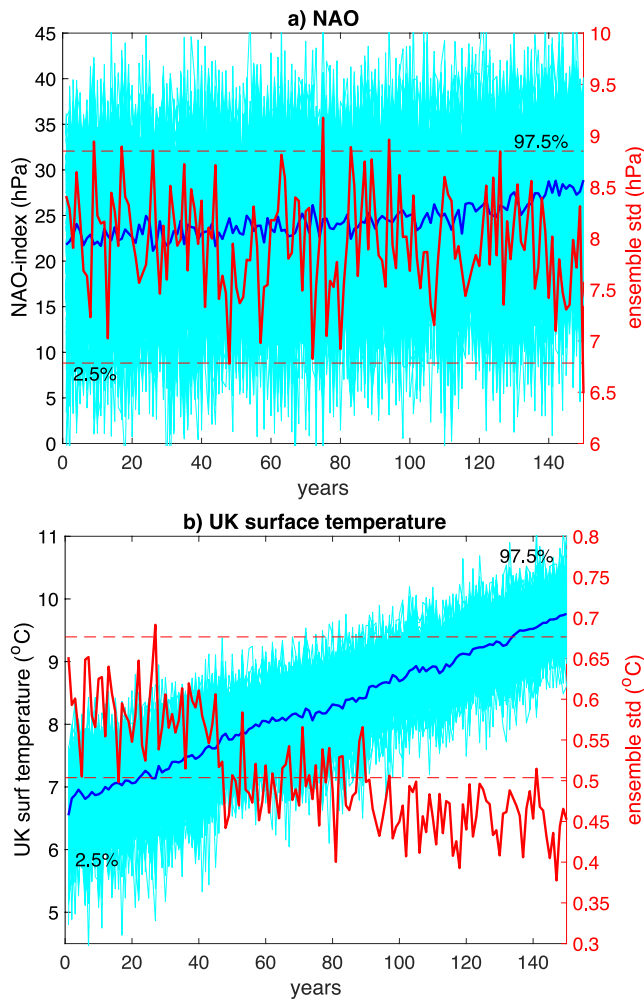
Figure 1. Ensemble mean (blue, left axis) and ensemble standard deviation (red, right axis) as functions of simulation years for the NAO-index (hPa; top panel) and the UK near-surface air temperature (°C; bottom panel), obtained from the 100-member 1%CO$_2$ ensemble. Also shown are time series obtained from individual ensemble members (cyan, left axis), in the same unit as the respective ensemble mean. The dashed lines indicate, for the standard deviation of 100 values randomly chosen from a 2,000-year control simulation, the 2.5%- and 97.5%-percentile, respectively. The range between the 2.5%- and 97.5%-percentile corresponds the range in which the standard deviation obtained from 100 values will lie in with 95% likelihood due to sampling variability. This range is 2.07 hPa for NAO-index and 0.17°C for UK surface temperature.

for discretized oscillatory processes, X_n, with similar assumptions, the ES of X_n, $h_n(\omega_j)$ at time step n and frequency ω_j, is approximately given by $|y_{n,\omega_j}|^2$.

The ES density, $h_n(\omega)$, is a function of time step n and frequency ω, and its exact time- and frequency-dependence is controlled by the filter g_m. In fact, $h_n(\omega)$ can be considered to describe the spectral content of the process in the neighborhood of time step n, with the size of the "neighborhood" being specified by the width of g_m. Since a filter g_m with a small width operates only locally on x_n (see Equation 1), we can choose the width of g_m to be as small as possible to assure a high degree of resolution in the time domain. However, if the width of g_m is made too small, we would not resolve anything in the frequency domain. On the other extreme, using a filter width that covers the entire time domain would resolve many frequencies but provide no resolution in time. In other words, it is not possible to get a high resolution in both the time and frequency domain. This is the so-called uncertainty principle (SI-A.1) that we are confronted with when studying nonstationary spectra. Thus, the key to define ES in a meaningful way is to choose a proper g_m, which allows a description of some-time dependence of spectral properties while simultaneously resolving some frequencies in the frequency domain. The choice of g_m needs to be made in relation to the characteristic time scale of the modulating amplitudes of oscillatory functions used to represent the nonstationary process X_n. More specifically, the width of g_m should be much shorter than the characteristic time scales of the modulating amplitudes of oscillatory functions used to represent X_n.

We define PES as a special case of ES. Similar to ES, PES are defined for oscillatory processes. A PES density, $h_n(\omega)$, is obtained by replacing the linear filter g_m by a simple box window corresponding to an interval I_n, where the subscript n indicates the central time step of the interval I_n. The box window has unit weights inside and zero weights outside the window. With this filter, we obtain a PES that evolves with n. Within the neighborhood of time step n, or more precisely within interval I_n, the variations of the modulating amplitudes of oscillatory functions are assumed to be negligible, and the process is considered as if it is stationary. For the 1%-CO$_2$ experiment, we assume that the modulating amplitudes of the oscillatory functions vary on time scales much longer than a couple of decades such that when we choose a time interval, I_n, of length 20 years, then the time series within I_n can be considered as if they were realizations of stationary processes. Justification of this assumption will be presented at the end of this subsection.

Often, one has only a single experiment such that an assumption about the nonstationarity in second moments is difficult to validate. Fortunately, we are in possession of an ensemble containing 100 ensemble members. For the wintertime NAO-index (defined below) and the near-surface air temperature averaged over the UK, Figure 1 describes the non-stationarity in terms of ensemble statistics calculated from the 100-members 1%-CO$_2$ ensemble. Before evaluating the non-stationarity in the second moments, we provide an impression of the ensemble and of the non-stationarity in the first moment by plotting the time series obtained from individual ensemble members (cyan lines) and the ensemble mean as a function of simulation years (blue lines). We see that both the NAO-index and the UK surface temperature increase almost linearly with time in the 1% CO$_2$ experiment. However, the trend in the temperature is much stronger than that in the NAO-index.

The non-stationarity in variance is shown by the ensemble standard deviation as a function of simulation years (red lines in Figure 1). Note that the ensemble standard deviation in a given year is calculated from

ensemble anomalies in that year, defined as the deviations of each ensemble member from the respective ensemble mean for that year (blue lines in Figure 1). Thus, any non-stationarity in the variance is independent of the non-stationarity in the mean. For both NAO-index and the UK surface temperature, the ensemble standard deviation varies strongly with time. This variation is due to sampling rather than representing a non-stationarity in standard deviation. This sampling variation is quantified using the 2000-years control simulation performed with the same climate model, which has stationary statistics. The dashed lines in Figure 1 are the 2.5%- and 97.5%-percentile obtained from standard deviations, each calculated using 100 NAO-indices or 100 UK surface temperatures randomly selected from the control simulation. The range between the two dashed lines indicates the 95% confidence interval, within which with 95% likelihood, the stationary standard deviation lies in. The 95% confidence interval amounts to 2.07 hPa for the NAO-index and 0.17°C for the UK temperature.

Since the statistics are stationary in the control simulation, the null-hypothesis of no-change in standard deviation can be rejected at 5%—significance level if the ensemble standard deviation in 1% CO_2 experiment lies outside the range indicated by the dashed lines. We see that the null-hypothesis can be rejected for the UK surface temperature, but not for the NAO-index, indicating that the variance is essentially stationary for NAO-index, but nonstationary for UK surface temperature. The non-stationarity is characterized by a decrease in standard deviation of about 0.2°C in 150 years, which is slightly larger than the 95% confident interval range of about 0.17°C. The decrease in standard deviation is gradual with a trend of about -0.12°C per century.

Figure 1b shows changes in the ensemble standard deviation occurring within short time intervals. An example is the large decrease of about 0.16°C occurring from year 45 to 48. However, these changes are generally smaller than the 95% confidence interval of about 0.17°C and hence lie well within the range of the sampling-induced variability found in the control simulation. This result justifies our assumption that when considering time series from a 1% CO_2 experiment as an oscillatory process represented by oscillatory functions, the modulating amplitudes of oscillatory functions vary on time scales much longer than a couple of decades, meaning that time series within 20-years intervals can be considered as if they are realizations of stationary processes.

2.2. Estimating PES Using Ensemble Periodogram

We estimate PES using an ensemble—a powerful aid not available for previous studies on nonstationary spectra. Priestley estimates ES using a weighting function without an ensemble to reduce sample fluctuations (Section A.2 in SI). In our case, the weighting function of Priestley is replaced by an ensemble average.

Consider an ensemble of size M. We denote the raw periodogram derived from the i-th ensemble member in interval I_n by $P_n^i(\omega)$, and an estimator of the PES by $\widehat{h_n(\omega)}$. We estimate PES as the ensemble-averaged periodogram defined by

$$\widehat{h_n(\omega)} = \frac{1}{M}\sum_{i=1}^{M} P_n^i(\omega). \tag{2}$$

The efficiency of ensemble averaging in reducing sample fluctuations to produce consistent spectral estimators is shown by Figure 2a (compare dotted curves and black dashed curve). In a similar fashion, piecewise evolutionary cross spectra and the related coherence and phase spectra can be estimated using the ensemble-averaged cross-periodograms and ensemble-averaged periodograms. Hereafter, PES (both the power spectra and the cross spectra and the related phase and coherence spectra) in an interval I_n are estimated using the respective ensemble periodograms, obtained by averaging over raw periodograms/cross-periodograms of individual members in I_n.

Since applying a weighting function (as suggested by Priestley) can smear out the temporally evolving features that one wants to address, the ES obtained using a weighting function are generally difficult to interpret. Replacing the weighting function with ensemble periodogram allows an easier interpretation, in which two time-varying features are clearly separated. One feature results from the short-term variations (shorter than the length of I_n) and is represented by the ensemble periodogram derived for the interval I_n
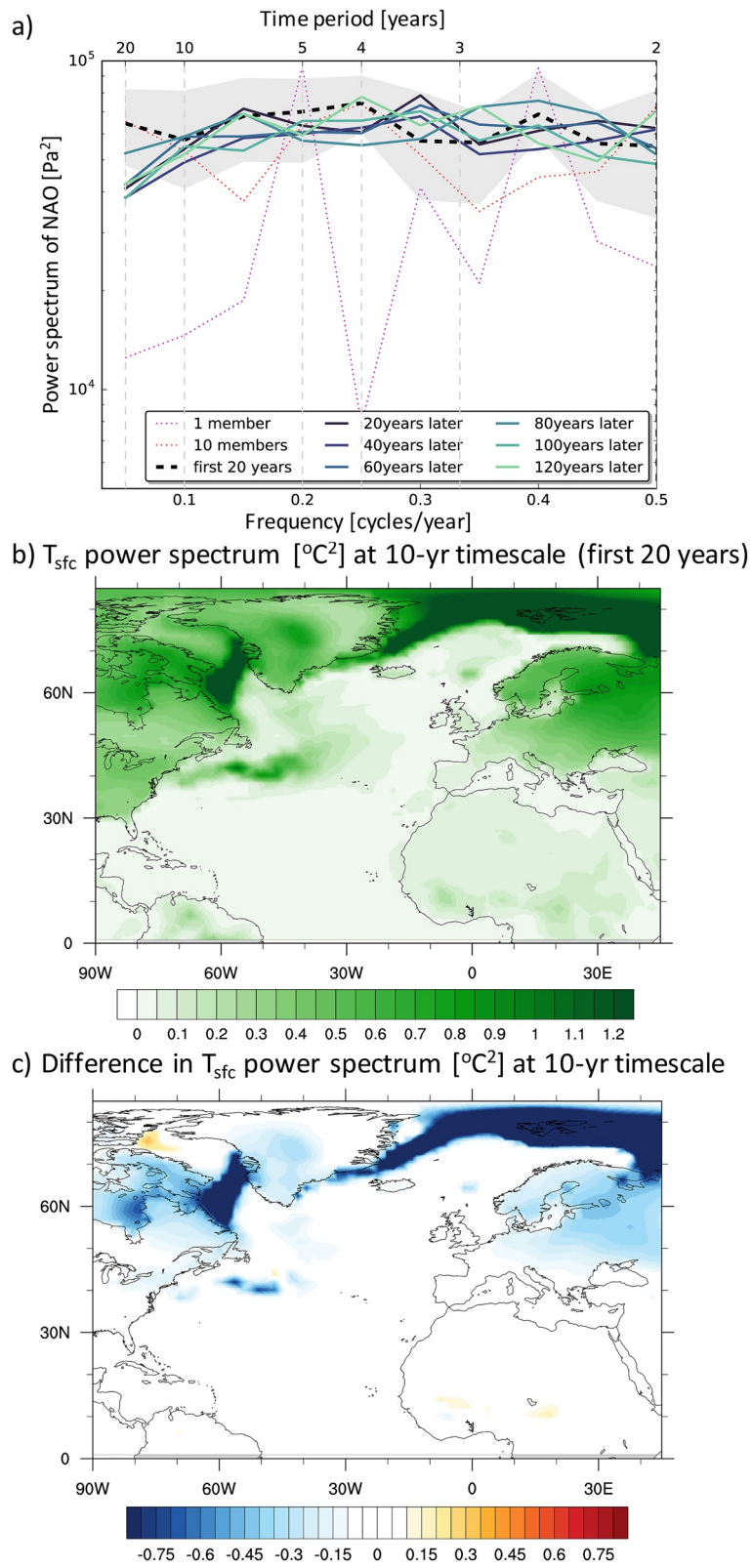
a)

b) T_{sfc} power spectrum [$^oC^2$] at 10-yr timescale (first 20 years)

c) Difference in T_{sfc} power spectrum [$^oC^2$] at 10-yr timescale

Figure 2

without involving any other intervals. The ensemble periodogram describes a frequency decomposition of the near-stationary variance within interval I_n. The other feature results from the slow nonstationary changes of the short-term variations, essentially providing the long-term time-dependence of the PES that is represented by the temporal evolution of the ensemble periodograms from interval to interval.

As a case study, we apply our PES to study the boreal wintertime (December-January-February [DJF]) relationship between NAO and surface temperature. The NAO is described by the sea level pressure difference between Lisbon, Portugal, and Stykkisholmur/Reykjavik, Iceland (Hurrell, 1995). For all ensemble members and all 20-year intervals, linear trends are removed before deriving the respective periodograms. This ensures that the periodogram estimates are not affected by possible linear trends associated with the non-stationarity in the first moment. For spatial pattern changes, we concentrate on the first and the last 20-year interval of the 1%-ensemble since we are interested in the largest possible change in the NAO-temperature relation in response to CO_2 forcing.

3. Spectra of NAO and Surface Temperature

The PES of NAO (Figure 2a; dark to light curves) is essentially white on short timescales (shorter than and equal to 20 years), which is consistent with previous studies (Gámiz-Fortis et al., 2002; Hurrell & Van-Loon, 1997; Rogers, 1984; Stephenson et al., 2000). The slow nonstationary changes as described by the PES of NAO in seven consecutive 20-year intervals are hardly noticeable from one interval to the next. Note that Figure 2a also illustrates the strong reduction of sampling fluctuations by estimating the PES using ensemble periodograms obtained from 100 (black dashed) ensemble members, compared to those obtained from one (magenta dotted) and 10 (red dotted) ensemble members. The differences in PES in later 20-year intervals relative to that in the first 20-year interval are tested against the null hypothesis that these differences are zero. The respective null-distribution is empirically estimated using the difference between two 100-member-averaged periodograms derived by randomly chosen 20-year periods from the long PI-control simulation. The respective 2.5% and 97.5% confidence bounds of this distribution are shown as the gray band centered around the PES in the first 20-year interval in Figure 2a. Except for a few spectral values (e.g., the one for the PES in the 5-th interval on a timescale of 4 years), most NAO spectra do not significantly change on all time scales shorter than 20 years. Only the spectral value on the 20-year timescale is slightly lower in a statistically significant manner in most of the later 20-year intervals than in the first 20-year interval. We hence conclude that with increasing global warming, the NAO variability remains essentially white. Except for a slight weakening in NAO variability on the 20-year timescale, the NAO variability on timescales shorter than 20 years remains at about the same level independent of the degree of the warming.

We apply the same approach to quantify the PES of boreal winter (DJF) surface temperature over the North Atlantic and surrounding continents, concentrating on the first and last 20-year interval changes. Figure 2b shows the spectral variance on the decadal timescale derived from the first 20-year interval. Large decadal spectral variance is found over the high-latitude lands surrounding the North Atlantic, reflecting that the variability of wintertime surface temperature is much stronger over high-latitude land than over the adjacent open ocean. Over land, particularly on the European continent, there is larger decadal variability over Northern and Eastern Europe compared to western and southern Europe that is dampened by its closer proximity to the ocean. Over ocean grid-cells, the largest decadal variance is found over the Labrador Sea, and over the Greenland and Barent Seas, which can be further associated with sea-ice cover variability (Kolstad & Screen, 2019). Over the North Atlantic, a maximum of spectral variance is found over the Gulf Stream, a frontal region with strong temperature gradients (Groth et al., 2017; McCarthy et al., 2018; Siqueira & Kirtman, 2016). This distribution with a similar strength is also found for spectral variances at other time scales (not shown), suggesting that the DJF surface temperature is essentially white. For the last 20-year interval, a reduction in decadal spectral variance tends to occur over regions that originally had high

Figure 2. (a) Piecewise evolutionary spectra (PES) of NAO for seven consecutive 20-year intervals (thick lines), estimated by ensemble periodograms. For the first 20-year interval, estimates derived from one single member (thin magenta dotted line), averaged over 10 members (thin red dotted line) are also shown. Gray shaded region marks the 2.5% and 97.5% confidence bounds for changes between the PES obtained from the first and the later 20-year intervals. (b) PES of surface temperature on decadal timescale for the first 20-year interval. (c) Difference in PES on decadal timescale between the last and the first 20-year intervals. Color shading is only provided for regions that have statistically significant difference (at 5% significant level).
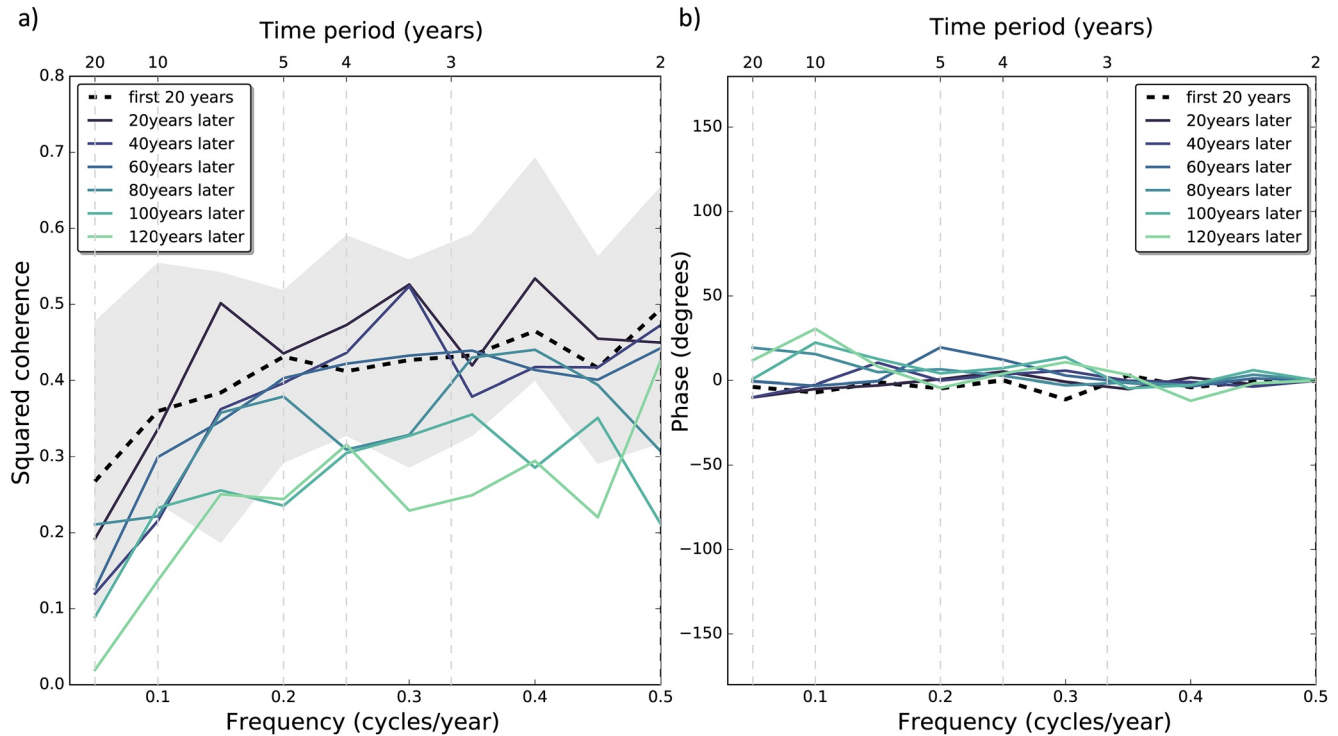
Figure 3. (a) Piecewise evolutionary coherence (PEC) between NAO and area-averaged UK surface temperature based on average over 100 members for the seven 20-year intervals. Gray shaded region marks the 2.5% and 97.5% confidence bounds for changes between the PEC obtained from the first and the later 20-year intervals. Outside these bounds, change in PEC is statistically significant at 5% significant level; (b) PEP spectra corresponding to (a). PEP, Piecewise evolutionary phase.

variability (Figure 2c), especially over the Labrador Sea and over the Greenland and Barent Seas. This reduction in decadal variance is likely due to sea-ice loss in a 4K warmer world that leaves these seas ice-free, thereby decreasing surface temperature variability. Significant reduction in decadal spectral variance is seen over eastern North America and most of northern Europe, which may be attributed to being in the nearby vicinity of now ice-free waters. In general, similar changes in the last relative to the first 20-year interval are found for spectral variances on other timescales.

4. Spectral Relations Between NAO and Surface Temperature

While the PES estimate of NAO does not change much in the 1% CO_2 experiment, it does not presuppose that the relationship of NAO with other climate quantities remains unchanged. We assess this by first evaluating the piecewise evolutionary coherence spectrum (hereafter PEC) between NAO and surface temperature over the United Kingdom (UK; averaged over 10W–0W, 50–60N) (Figure 3a). The PEC estimated from 100 ensemble members is between 0.25 and 0.5 in the first 20-year interval (black solid). Relative to the first 20-year interval, the PEC values on all timescales tend to systematically reduce after about 60–80 years, albeit not yet statistically significant. We test the difference between the PEC values in the later 20-year intervals and the PEC values in the first 20-year interval against the null hypothesis that the differences are zero. Akin to the test performed for PES, the null-distribution is empirically constructed using differences between two 100-member-averaged coherence spectra derived by randomly chosen 20-year intervals from the long control simulation. The respective 2.5% and 97.5% confidence bounds of this distribution are shown as the gray band centered around the PEC in the first 20-year interval in Figure 3a. After 100 years, hints of statistically significant reduction in PEC is seen on interannual timescales. In the last 20-year interval, PEC values are reduced to 0.1–0.2 at all resolved timescales. Unlike the PES of NAO (Figure 2a), the null-hypothesis that there is no change in PEC from the first to the last 20-year interval can be rejected on almost all resolved timescales (Figure 3a). The drop in PEC suggests that the regional influence of NAO on UK surface temperature is reduced in a warmer world on almost all timescales. Associated with the PEC is the piecewise
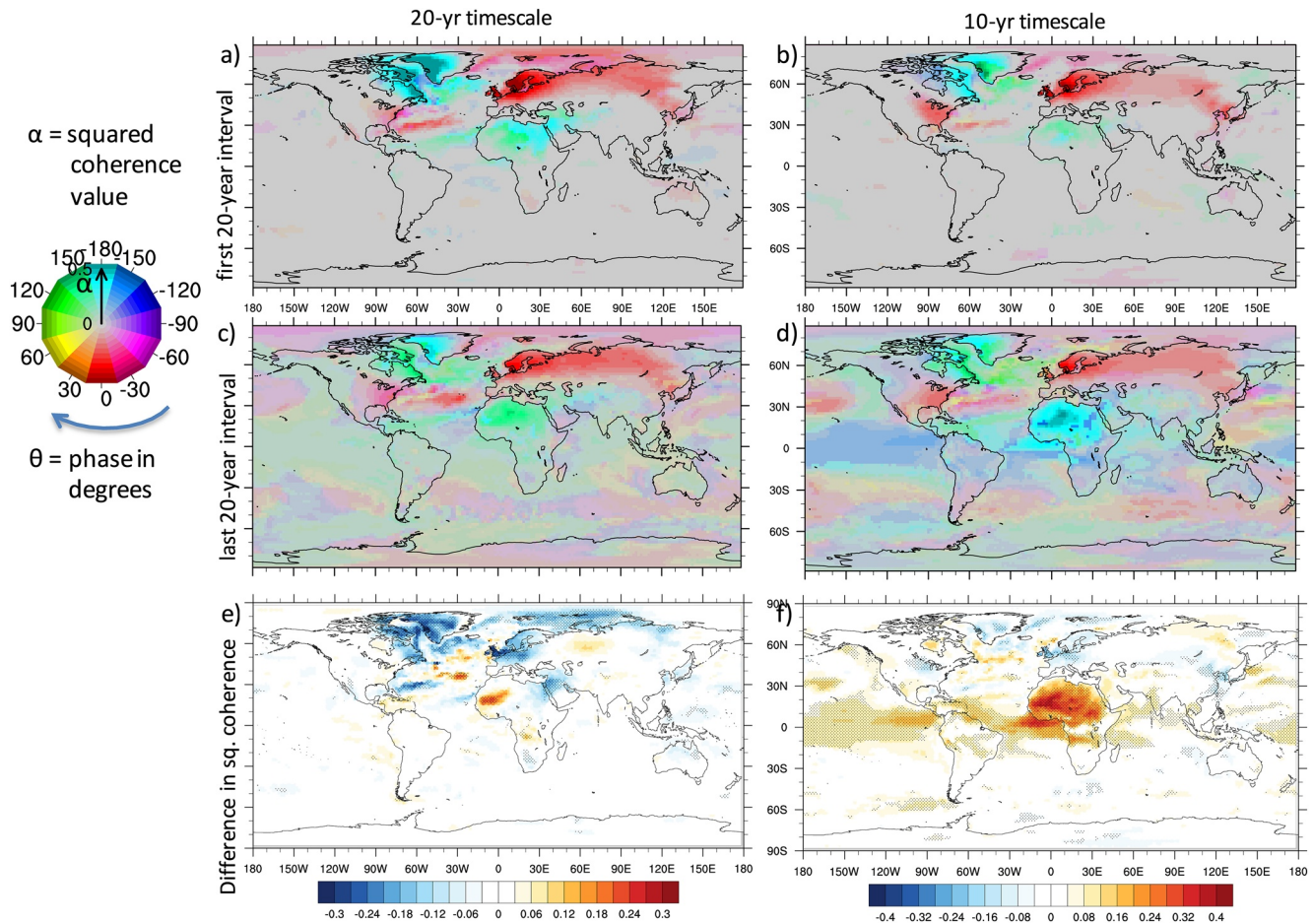
Figure 4. (a) PEC-pattern describing the coherence (saturation) and the phase in degrees (hue) between NAO and surface temperature on bi-decadal timescale for the first 20-year interval. (b) Same as (a) except for decadal timescale. (c) Same as (a) that is on bi-decadal timescale except for last 20-year interval. (d) Same as (b) that is on decadal timescale except for last 20-year interval. (e) Difference between PEC of NAO with surface temperature on bi-decadal timescale in the last and that in the first 20-year interval. Stippled regions mark changes in PEC in the last relative to that in the first 20-year interval, that are statistically significant at 5% significant level. (f) Same as (e) except for decadal timescale.

evolutionary phase spectrum (PEP) that provides a lead-lag information on the relation between the two quantities (Figure 3b). NAO and the surface temperature over the UK are essentially in-phase overall resolved timescales in the first 20-year interval (black dashed line). In general, the two variables remain by and large in-phase throughout of the experiment (dark to light lines), except for a slight increase in phase lag by roughly 30° on the decadal timescale.

We extend the calculation of PEC and PEP to NAO and surface temperatures everywhere on the globe, thereby producing spatial patterns of PEC- and PEP-values on various timescales in different 20-year intervals. For a given timescale and a given 20-year interval, the respective PEC- and PEP-values are combined and displayed in a so called PEC-pattern, with the phase being described by the hue and the squared coherence by the saturation. As an example, the PEC-pattern for the bi-decadal timescale in the first 20-year interval is illustrated in Figure 4a. The figure reflects how NAO is related to the surface temperature, with large in-phase squared coherence values over eastern continental United States and northern Europe (in-phase relation illustrated with red hue), and 180°-out-of-phase coherence values over eastern Canada, Greenland, and the region south of the Mediterranean (out-of-phase relation illustrated with turquoise hue). These phase relations are consistent with the large-scale circulation pattern associated with the positive winter-time NAO that draws cold polar air over eastern Canada and Greenland while bringing warm subtropical air toward northern Europe during the positive NAO phase (Hurrell, 1995; Hurrell & Deser, 2009; Hurrell et al., 2003). These phase relations are similar irrespective of timescale, as seen by comparing the

PEC-pattern on the bi-decadal timescale (Figure 4a) with that on the decadal timescale (Figure 4c). Furthermore, the overall structure of the phase relation does not change much with time for future projections, as suggested by comparing the PEC-pattern for the first (Figures 4a and 4c) with that for the last 20-year interval (Figures 4b and 4d).

The significant 180°-out-of-phase relation in Figure 4d suggests a tropical Pacific-Atlantic connection associated with the NAO. Previous studies have shown that El Niño is typically associated with negative NAO (Brönnimann, 2007; Mathieu et al., 2004), consistent with the out-of-phase relation between tropical Pacific and NAO (Figure 4d), albeit for a future projection. El Niño-like conditions can weaken the polar vortex and induce weaker Azores high (negative NAO pattern) (Rodríguez-Fonseca et al., 2016; van Loon & Lebitzke, 1987; van Loon & Madden, 1981). Weakened easterly trades during negative NAO phase (weaker Azores high) can reduce latent heat flux over the ocean and thereby warming sea surface temperatures (SST) in the tropical Atlantic (Giannini et al., 2021; Park & Li, 2019), reflecting an anti-phase relation between NAO and tropical Atlantic SST (Figure 4d). While both the relationship of tropical Pacific with NAO and that of tropical Atlantic with NAO are generally out-of-phase, note the bluer tinge of the phase relation between tropical Pacific and NAO compared to the turquoise out-of-phase color for tropical Atlantic/western Africa and NAO. The bluer tinge suggests that the tropical Pacific leads the NAO, possibly indicating ENSO-like modulation on the NAO.

We applied the same test for evaluating significance in the change of PEC between NAO and UK surface temperature to each grid point and find not only significant changes in squared coherence in some regions (stippled regions in Figures 4e and 4f), but that the changes in squared coherence are also disparate on different timescales. More specifically, in some regions, changes in squared coherence on bi-decadal timescales differs from those on timescales shorter than 20 years. On the 20-year timescale, significant decrease in PEC is seen at high northern latitudes (Figure 4e), especially over northern Europe, eastern Canada, western Greenland, and Barents and Kara seas. This decrease could be related to sea-ice retreat. The proximity to sea ice induces high variability of surface temperature. However, as sea-ice coverage gradually diminishes with increasing GHG, ice-free water could dampen the overlying and surrounding surface temperature variability.

On timescales shorter than 20 years, much of the decrease in PEC at high northern latitudes is muted (Figure 4f), except for a small region near the UK where the reduction of the in-phase squared coherence between NAO and the surface temperature is weaker than elsewhere, consistent with Figure 3a. It is curious that the strong and significant decline in PEC at high northern latitudes is only on bi-decadal timescales (Figure 4e), and not so much on the shorter timescales (Figure 4f). Even though the damping of the ice-free ocean on surface temperature can affect the squared coherence on all timescales, the gradual diminishing of sea ice induced by sea-ice retreat can make the changes in PEC on the longest resolved timescale (i.e., bi-decadal timescale) more prominent. Further investigation is certainly needed to fully understand the cause for the weakening of this relationship on bi-decadal timescale.

The most noticeable changes in PEC on decadal timescale are found over the tropical and subtropical northern Africa, the tropical Atlantic, and even into the tropical Pacific (Figure 4f). Comparing Figure 4d with 4c suggests that the out-of-phase relation on decadal timescales is strongly increased over the tropical Atlantic and Pacific, and the Sahel region in the last 20-year interval, which corresponds to the increased squared coherence (Figure 4f). In general, the PEC between NAO and surface temperatures in the Sahel region tends to increase on timescales shorter than 20 years, while on bidecadal timescales, it is effectively zero (Figure S1). We speculate that the increase in squared coherence could be related to the weakening of the Hadley cell strength projected by the 1%-CO_2 ensemble (Reimann & von Storch, 2020), which may allow more mid-latitude disturbances to pass through. As a consequence, surface temperature variability in the tropics and subtropics become more strongly related to large-scale mid-latitude circulation and eventually to NAO, leading to an increase in the squared coherence there. Further investigation is needed to verify the impact of the change in the Hadley circulation strength on the relationship between NAO and surface temperature in the tropical and subtropical regions.

5. Summary and Discussion

We use PES—a special case of Priestley's ES—derived from ensemble periodograms to investigate changes in spectra and spectral-relation patterns of climate variables in a warming climate. We emphasize the need for an ensemble to obtain the estimates of PES, not only because a large ensemble is required to make the estimates consistent and efficient. An ensemble is also a natural means for dealing with nonstationary processes. Such an ensemble is not available from observations, but must be generated using numerical models. For a selected warming stage common to all ensemble members, piecewise evolutionary coherence spectra (PEC) and piecewise evolutionary phase spectra (PEP) obtained from ensemble periodograms provides us with global PEC-patterns on various timescales at this warming stage. Comparing these patterns obtained for different warming stages allows us to evaluate how the spectral relations on different time scales evolve in different parts of the world from one warming stage to another.

This whole approach is applied to the wintertime NAO-index and the wintertime near-surface air temperature. We find that while the variability of both NAO and surface temperature remains essentially white with increasing GHG forcing, the spectral relation of NAO to surface temperatures in various regions of the world can change. Moreover, changes in these spectral relations reveal different spatial distributions, depending on the timescale of choice. On the bi-decadal timescale, the longest resolved timescale, strong reduction in PEC between NAO and surface temperatures are concentrated over high-latitude lands surrounding the northern North Atlantic. However, on shorter timescales, significant increases in PEC between NAO and surface temperature are found in the tropical and subtropical regions of North Africa, and the tropical Atlantic and Pacific. The result that spectral relations on different timescales can change disparately at different stages of the warming shed new light on the influence of NAO on regional climate and could further improve future regional climate predictions.

The definition of both ES and PES relies on the assumption that the nonstationary process under consideration can be represented by oscillatory functions. This means for PES defined for intervals I_n that the modulating amplitudes of the oscillatory functions must vary on time scales longer than the length of I_n. At least for the NAO-index and the near-surface air temperature obtained from an ensemble of 1% CO_2 experiments, the modulating amplitudes do not vary significantly on time scales shorter than a couple of decades so that it is reasonable to choose the length of interval I_n to be 20 years. Generally, if the modulating amplitudes vary strongly on short timescales, it is difficult to find an interval I_n or more generally a linear filter g_m, which has a sufficiently large width to ensure a good resolution in frequency domain. The definition of both PES and ES becomes inappropriate. Other approaches that do not rely on oscillatory functions would then be needed. We expect that more and further improved approaches will come, as studying nonstationary spectra in the context of climate change climate is still in its infancy.

Data Availability Statement

Data used in this study is from the Max Planck Institute - Grand Ensemble, which is available on https://esgf-data.dkrz.de/projects/mpi-ge/.

References

Brönnimann, S. (2007). Impact of El Niño Southern Oscillation on European climate. *Reviews of Geophysics*, *45*(3). https://doi.org/10.1029/2006RG000199

Deser, C., Hurrell, J. W., & Phillips, A. S. (2017). The role of the North Atlantic Oscillation in European climate projections. *Climate Dynamics*, *49*(9), 3141–3157. https://doi.org/10.1007/s00382-016-3502-z

Deser, C., Phillips, A., Bourdette, V., & Teng, H. (2012). Uncertainty in climate change projections: The role of internal variability. *Climate Dynamics*, *38*(3), 527–546. https://doi.org/10.1007/s00382-010-0977-x

Fyfe, J. C., Derksen, C., Mudryk, L., Flato, G. M., Santer, B. D., Swart, N. C., et al. (2017). Large near-term projected snowpack loss over the western United States. *Nature Communications*, *8*(1), 14996. https://doi.org/10.1038/ncomms14996

Gámiz-Fortis, S. R., Pozo-Vázquez, D., Esteban-Parra, M. J., & Castro-Díez, Y. (2002). Spectral characteristics and predictability of the NAO assessed through singular spectral analysis. *Journal of Geophysical Research*, *107*(D23), ACL111–ACL1115. https://doi.org/10.1029/2001JD001436

Giannini, A., Cane, M. A., & Kushnir, Y. (2001). Interdecadal Changes in the ENSO Teleconnection to the Caribbean Region and the North Atlantic Oscillation. *Journal of Climate*, *14*(13), 2867–2879. https://doi.org/10.1175/1520-0442(2001)014<2867:icitet>2.0.co;2

Groth, A., Feliks, Y., Kondrashov, D., & Ghil, M. (2017). Interannual variability in the North Atlantic Ocean temperature field and its association with the wind stress forcing. *Journal of Climate*, *30*(7), 2655–2678. https://doi.org/10.1175/JCLI-D-16-0370.1

Hurrell, J. (1995). Decadal trends in the North Atlantic Oscillation: Regional temperatures and precipitation. *Science*, *269*(5224), 676–679. https://doi.org/10.1126/science.269.5224.676

Hurrell, J., & Deser, C. (2009). North Atlantic climate variability: The role of the North Atlantic Oscillation. *Journal of Marine Systems*, *78*(1), 28–41. https://doi.org/10.1016/j.jmarsys.2008.11.026

Hurrell, J., Kushnir, Y., Ottersen, G., & Visbeck, M. (2003). An overview of the North Atlantic oscillation. *The North Atlantic Oscillation: Climatic significance and environmental impact*, Geophysical Monograph Series, 134, 1–35. AGU. https://doi.org/10.1029/134GM01

Hurrell, J., & Van Loon, H. (1997). Decadal variations in climate associated with the North Atlantic Oscillation. *Climatic Change*, *36*(3–4), 301–326. https://doi.org/10.1023/A:1005314315270

Kay, J. E., Deser, C., Phillips, A., Mai, A., Hannay, C., Strand, G., et al. (2015). The Community Earth System Model (CESM) large ensemble project: A community resource for studying climate change in the presence of internal climate variability. *Bulletin of the American Meteorological Society*, *96*(8), 1333–1349. https://doi.org/10.1175/BAMS-D-13-00255.1

Kolstad, E. W., & Screen, J. A. (2019). Nonstationary relationship between autumn Arctic sea ice and the winter North Atlantic Oscillation. *Geophysical Research Letters*, *46*(13), 7583–7591. https://doi.org/10.1029/2019GL083059

Maher, N., Matei, D., Milinski, S., & Marotzke, J. (2018). ENSO change in climate projections: Forced response or internal variability? *Geophysical Research Letters*, *45*(20), 11390–11398. https://doi.org/10.1029/2018GL079764

Maher, N., Milinski, S., Suarez-Gutierrez, L., Botzet, M., Dobrynin, M., Kornblueh, L., et al. (2019). The Max Planck Institute Grand Ensemble: Enabling the exploration of climate system variability. *Journal of Advances in Modeling Earth Systems*, *11*(7), 2050–2069. https://doi.org/10.1029/2019MS001639

Manzini, E., Karpechko, A. Y., & Kornblueh, L. (2018). Nonlinear response of the stratosphere and the north Atlantic-European climate to global warming. *Geophysical Research Letters*, *45*(9), 4255–4263. https://doi.org/10.1029/2018GL077826

Mathieu, P. P., Sutton, R. T., Dong, B. W., & Collins, M. (2004). Predictability of winter climate over the North Atlantic European region during ENSO events. *Journal of Climate*, *17*(10), 1953–1974. https://doi.org/10.1175/1520-0442(2004)017<1953:POWCOT>2.0.CO;2

McCarthy, G. D., Joyce, T. M., & Josey, S. A. (2018). Gulf Stream variability in the context of quasi-decadal and multidecadal Atlantic climate variability. *Geophysical Research Letters*, *45*(20), 11257–11264. https://doi.org/10.1029/2018GL079336

Milinski, S. (2019). *Internal variability in a changing climate: A large ensemble perspective on tropical Atlantic rainfall* (Doctoral dissertation). Universität Hamburg. https://doi.org/10.17617/2.3165869

Park, J.-H., & Li, T. (2019). Interdecadal modulation of El Niño–tropical North Atlantic teleconnection by the Atlantic multi-decadal oscillation. *Climate Dynamics*, *52*(9), 5345–5360. https://doi.org/10.1007/s00382-018-4452-4

Priestley, M. B. (1965). Evolutionary spectra and non-stationary processes. *Journal of the Royal Statistical Society: Series B*, *27*(2), 204–229. https://doi.org/10.1111/j.2517-6161.1965.tb01488.x

Priestley, M. B. (1967). Power spectral analysis of non-stationary random processes. *Journal of Sound and Vibration*, *6*(1), 86–97. https://doi.org/10.1016/0022-460X(67)90160-5

Priestley, M. B. (1981). *Spectral analysis and time series*. London: Academic Press.

Priestley, M. B. (1988). *Non-linear and non-stationary time series analysis*. London: Academic Press.

Reimann, L., & von Storch, J.-S. (2020). A phase space consideration of changing climate pdf. *Climate Dynamics*, *54*, 2633–2662. https://doi.org/10.1007/s00382-020-05130-8

Rodgers, K. B., Lin, J., & Frölicher, T. L. (2015). Emergence of multiple ocean ecosystem drivers in a large ensemble suite with an Earth system model. *Biogeosciences*, *12*(11), 3301–3320. https://doi.org/10.5194/bg-12-3301-2015

Rodríguez-Fonseca, B., Suárez-Moreno, R., Ayarzagüena, B., López-Parages, J., Gómara, I., Mohino, E., et al. (2016). A review of ENSO influence on the North Atlantic. A non-stationary signal. *Atmosphere*, *87*(7), 87. https://doi.org/10.3390/atmos7070087

Rogers, J. C. (1984). The association between the North Atlantic Oscillation and the Southern Oscillation in the Northern Hemisphere. *Monthly Weather Review*, *112*(10), 1999–2015. https://doi.org/10.1175/1520-0493(1984)112<1999:tabtna>2.0.co;2

Shepherd, T. G. (2014). Atmospheric circulation as a source of uncertainty in climate change projections. *Nature Geoscience*, *7*(10), 703–708. https://doi.org/10.1038/ngeo2253

Siqueira, L., & Kirtman, B. P. (2016). Atlantic near-term climate variability and the role of a resolved Gulf Stream. *Geophysical Research Letters*, *43*(8), 3964–3972. https://doi.org/10.1002/2016GL068694

Stephenson, D., Pavan, V., & Bojariu, R. (2000). Is the North Atlantic Oscillation a random walk? *International Journal of Climatology*, *20*(1), 1–18. https://doi.org/10.1002/(sici)1097-0088(200001)20:1<1::aid-joc456>3.0.co;2-p

van Loon, H., & Lebitzke, K. (1987). The Southern Oscillation. Part V: The anomalies in the lower stratosphere of the northern hemisphere in winter and a comparison with the Quasi-Biennial Oscillation. *Monthly Weather Review*, *115*(2), 357–369. https://doi.org/10.1175/1520-0493(1987)115<0357:TSOPVT>2.0.CO;2

van Loon, H., & Madden, R. A. (1981). The Southern Oscillation. Part I: Global associations with pressure and temperature in northern winter. *Monthly Weather Review*, *109*(6), 1150–1162. https://doi.org/10.1175/1520-0493(1981)109%3C1150:TSOPIG>2.0.CO;2